

Non-linear tensile creep of polypropylene: Time-strain superposition and creep prediction

Jan Kolařík^{a,*}, Alessandro Pegoretti^b

^a Department of Materials, Institute of Macromolecular Chemistry, Academy of Sciences of the Czech Republic, 162 06 Prague 6, Czech Republic

^b Department of Materials Engineering and Industrial Technologies, University of Trento, 38050 Trento, Italy

Received 5 May 2005; received in revised form 1 November 2005; accepted 3 November 2005

Available online 21 November 2005

Abstract

In most practical applications, isothermal compliance of polymeric materials depends on both time and stress so that their non-linear viscoelastic behavior is of primary importance. A concept is adopted that the non-linearity of tensile creep is mainly brought about by the strain-induced increment of the free volume (in materials with Poisson ratio smaller than 0.5). Consequently, the traditional stress-strain linearity limit can be viewed as an artificial limit related to limited accuracy of the measurements at low stresses and strains. The internal time—tensile compliance superposition of non-linear creep data is applied to construct a generalized compliance curve, which corresponds to a pseudo iso-free-volume state. The superposition of compliance curves obtained at different stresses requires shift factors along the time axis calculated a priori for individual data points. As the generalized curve can be generated by means of short-term creeps, the proposed procedure offers essential savings of experimental time. A most practical outcome of the outlined format is that the generalized dependence can be employed for predicting the real time-dependent compliance for any stress in the range of reversible strains. The results indicate that the compliance of PPs decreases with their crystallinity, while their creep rates are almost identical. Only rubber-toughened PP does show a slightly higher creep rate, which is attributed to the ‘softening’ effect of rubber particles in the PP matrix.

© 2005 Elsevier Ltd. All rights reserved.

Keywords: Polypropylene; Tensile creep; Free volume

1. Introduction

The dimensional stability of thermoplastics exposed to a constant load for a period of time corresponds to their resistance to creep [1]. The acquisition of creep data and their quantitative analysis, extrapolation and/or prediction are still urgent tasks of materials research. The creep behavior of many industrially important polymers has already been described in many papers, which are reviewed in Refs. [2,3]. To date, creep behavior of polymeric materials has mostly been reported in a graphical form as documented in an extensive collection [2]. When experimental data can be fitted by a suitable equation, their storage and subsequent characterization of the creep process are facilitated. However, proposed equations are mainly empirical and their validity may be limited to particular materials and/or test conditions.

Theoretical background of the creep behavior of polymers has been well elaborated in the framework of the linear viscoelasticity [4–11]. This theory assumes that compliance (or modulus) is a function of time, but not of stress or strain. Ideally, materials are assumed to be homogeneous and rheologically simple and imposed deformations are infinitesimally small. However, polymeric materials used in practice are usually heterogeneous and rheologically complex and produced deformations are far from being infinitesimal. A characteristic feature of most thermoplastics, particularly of partially crystalline ones, is a very low limit of the linear stress–strain relationship, say a few of tenths of percent [12]. For instance, identical creep compliance responses of polymeric materials were observed for strains less than 0.2% [13]. Beyond this limit, isothermal compliance (or modulus) becomes a function of both time and stress (or strain). Anyway, non-linear viscoelastic behavior occurs over a major portion of the entire response interval of most polymeric materials and plays a key role in most applications. Quantitative data analysis in the non-linear region is much more difficult than in the linear region and

* Corresponding author. Tel.: +420 296 809 330; fax: +420 296 809 410.
E-mail address: kolarik@imc.cas.cz (J. Kolařík).

requires a deeper understanding of the underlying processes controlling the mechanical response [6,7,11–28].

Recent approaches to non-linear viscoelasticity of polymers mostly use the concept of a ‘material clock’ to describe how the instantaneous rate of retardation (or relaxation) is controlled by the current state of the material in the course of a solicitation. In this concept, the internal time of a material differs from the laboratory time. The shift factor is introduced to convert the experimental time into the internal time in a reference state of the material. The proposed quantities controlling a material clock are, e.g. free volume [13,18–20,23,25,26,29–31], strain [13] or stress [32]. Probably the most useful of these concepts is that of the free volume with regard to the fact that the phenomenological theory of viscoelasticity [4–11] has shown that retardation (or relaxation) times are controlled by the free volume available for molecular (segmental) motions in polymeric materials. It is generally known that an isotropic solid body with Poisson’s ratio $\nu < 0.5$ dilates when deformed in tension [7–11]. As the strain-induced increase in specific volume can be identified with the increase in free volume [33–35], the molecular mobility in polymers is markedly tensile strain-dependent. An analogous acceleration of creep or relaxation in the case of shear (or torsion) deformations, which are presumed not to be accompanied by mechanically induced volume dilatation, is still a matter of dispute [20]. To capture the non-linear behavior under shear-dominated loading, the free volume approach was formally modified by assuming that also an imposed shear deformation results in a restructuring of the polymer chains and thus accounts for enhancement of molecular mobility [13,25]. Although this generalized approach was formally quite successful, physical meaning of the parameters associated with the distortional effects is to be clarified.

Recently, a thermodynamic theory of the non-linear viscoelasticity of glassy polymers has been proposed [36] and applied to their yield mechanism [37]. Using the concept of the Gibbs energy density increasing on reversible deformations, the authors generalized the time–temperature superposition in the form of the time–deformation–temperature superposition. Another thermodynamically consistent, non-linear viscoelastic approach has been proposed for modeling glassy polymers [38,39], which introduces the configurational internal energy as an alternative material clock. However, both models are extremely complex and their application to a specific material would require a high number of various material parameters (up to 29 in Ref. [39]) from independent experiments. So far the models have not been modified and verified for creep experiments.

The creep behavior of polypropylene (PP), which ranks among the most used thermoplastics, has been studied in a series of papers [2,3,12,29,30,40–46]. As the reported stress-strain linearity limit of PP is very low, creep measurements under this limit are inaccurate and impractical because they do not provide data useful for practice. Applying the free volume approach to the non-linear tensile creep of PP [3] and of the PP/SAN [29] or PP/cycloolefin copolymer blends [30], we have derived a formula for the shift factor, which allows to construct

a generalized creep curve over a long time interval by using the time-tensile strain superposition. In this comparative study, we have adopted the developed format to analyze the effect of the composition and crystallinity of six different species of commercial PPs on their creep behavior. It is important to realize that the non-linear creep may develop a critical material property in many applications. Our objectives are (i) to quantitatively describe the non-linear creep behavior by introducing a set of material parameters, (ii) to compare generalized compliance curves of studied PPs constructed for a pseudo iso-free-volume state by superposing data obtained for various stresses and (iii) to employ the generalized creep curves for prediction of the real time-dependent compliance for a selected stress (lower than the yield stress).

2. Theoretical background

As the strain-induced volume increment of the materials can be identified with an increment in the free volume [33–35], increasing strain in the tensile creep accounts for an increase in molecular mobility and a perceptible shortening of retardation times. However, quantification of this concept suffers from a series of approximations, because ‘auxiliary’ quantities occurring in the derived equations are difficult to determine.

2.1. Empirical function for fitting the creep of polypropylene

The strain in tensile creep, $\varepsilon(t, \sigma, T)$, depending on time t , stress σ and temperature T , is usually viewed as consisting of three components: [1,6–11] (i) elastic (instantaneous, reversible) $\varepsilon_e(\sigma, T)$; (ii) viscoelastic (time-dependent, reversible) $\varepsilon_v(t, \sigma, T)$; (iii) plastic (irreversible) $\varepsilon_p(t, \sigma, T)$:

$$\varepsilon(t, \sigma, T) = \varepsilon_e(\sigma, T) + \varepsilon_v(t, \sigma, T) + \varepsilon_p(t, \sigma, T) \quad (1)$$

If no plastic deformation is produced in the course of creeping, the tensile compliance $D(t, \sigma) = \varepsilon(t, \sigma) / \sigma$ for the isothermal non-linear creep reads

$$D(t, \sigma) = D_e(\sigma) + D_v(t, \sigma) \quad (2)$$

It would be practical [7,47] to express the compliance as a product of independent functions of time, stress and temperature, i.e. $D(t, \sigma, T) = \text{const} \times g_1(t) g_2(\sigma) g_3(T)$. However, experimental results often indicate interrelations between these presumably independent functions. The Arrhenius equation is suitable for $g_3(T)$ at $T < T_g$, while the Williams–Landel–Ferry (WLF) equation is used [5,7] in the interval $T_g < T < T_g + 100$ K. Empirical equations proposed to fit $D(t, \sigma)$ of plastics were reviewed in Refs. [1,3,14,43,47]. Analogous functions were proposed for $D_v(t, \sigma)$, but there is no doubt that $D(t, \sigma)$ is a much more practical function for handling the creep behavior of polymeric materials. A relatively simple equation was found suitable for describing isothermal creep of polypropylene and its blends: [3,29,30,40].

$$\log D(t, \sigma) = \log W(\sigma) + n \log \left(\frac{t}{\tau_{rm}} \right) \quad (3)$$

where $W(\sigma)$ is a function of stress (usually can be approximated by the power law or hyperbolic sine [14]), τ_{rm} is the mean retardation time and $0 \leq n \leq 1$ is the shape parameter reflecting the distribution of retardation times. Indicated parameters are generally determined a posteriori by fitting experimental data. The spectrum of retardation times corresponding to the power function t^n can be found in Ref. [14].

2.2. Tensile creep as a non-iso-free volume process

The free volume concept provides a simple unifying basis for explaining the effects of temperature, hydrostatic pressure, tensile deformation, chain ends, diluents (plasticizers), the state of physical aging, etc. on the viscoelastic behavior of polymers. The dimensionless fractional free volume [4–8,10] is routinely defined as

$$f = \frac{(V - V_h)}{V} = \frac{V_f}{V} \quad (4)$$

where V is the specific volume, V_h is the specific volume occupied by molecules (extrapolated from the melt without change of phase [8]) and V_f is the free volume. The free volume is presumed [4,35] to consist of vacancies of about the same size as mobile molecular segments. The glassy state of polymers is generally viewed [4–8,10] as an iso-free-volume state with a fractional free volume $f_g = 0.025$ (the secondary relaxation processes associated with the motions of side chains or short segment of backbones account [48] for small changes in f_g). If solely the effects of temperature T and of time-dependent tensile strain $\varepsilon(t)$ in the region of reversible deformations are considered, the fractional free volume can be expressed as

$$\begin{aligned} f[T, \varepsilon(t)] &= f_g + \alpha_{fv}(T - T_g) + (1 - 2\nu)\varepsilon(t) \\ &= f_g + \Delta f_T + \Delta f_\varepsilon \end{aligned} \quad (5)$$

where α_{fv} is the expansion coefficient of the free volume at $T > T_g$ (which can be approximated as the difference between the expansion coefficients of the material above and below T_g , i.e. $\alpha_{fv} = \alpha_1 - \alpha_g$), ν is Poisson's ratio and $[(1 - 2\nu)\varepsilon(t)]$ is the strain-induced dilatation (terms including $\varepsilon(t)^2$ and $\varepsilon(t)^3$ are neglected). It is essential to note that an increase in the specimen volume by 1% due to tensile deformation, i.e. $\Delta f_\varepsilon = 0.01$, leads to free volume f at T_g . The latter is assumed to control retardation times τ_r according to the following equation [4,10,49]:

$$\ln \tau_r = \ln \Omega + \left(\frac{B}{f}\right) \quad (6)$$

where Ω is the frequency of thermal motion inside a potential well and B is a numerical factor related to the ratio of the volume of a jumping segment to the volume of critical vacancy necessary for the implementation of a segment jump (B is generally expected to be close to 1). The effect of f on τ_r is routinely expressed by means of the shift factor a along the time scale [3,10,17]:

$$\log a = \log \tau_r(f_2) - \log \tau_r(f_1) \quad (7)$$

where $f_2 > f_1$. The time-strain shift factor, $\log a_\varepsilon(t)$, defined as the ratio of the mean retardation time $\tau_{rm}[\varepsilon(t), T_c]$ at a strain $\varepsilon(t)$ and $\tau_{rmi}[\varepsilon_i = 0, T_c]$ for initial time $t_i = 0$ (at a constant temperature T_c) is obtained [3] by combining Eqs (5) and (7):

$$\log a_\varepsilon(t) = -(B/2.303) \frac{[(1 - 2\nu)M\varepsilon(t)/(f_g + \Delta f_{T_c})]}{[(1 - 2\nu)M\varepsilon(t) + (f_g + \Delta f_{T_c})]} \quad (8)$$

where M (derived in the next section) is the ratio of the average strain of the creeping phase (or component) in the multiphase test specimen and of measured strain. The values of $\log a_\varepsilon(t)$ needed for the time-strain superposition are to be calculated a priori as a function of $\varepsilon(t)$. In this strain-based formulation, $\log a_\varepsilon(t)$ is not a constant for an isostress creep curve, but grows from point to point with the creep strain due to increasing free volume in the creeping specimen. Thus $a_\varepsilon(t)$ is very different from the shift factor in the time-temperature superposition, which is constant for the whole isotherm creep curve and is obtained a posteriori by means of an empirical shift of the experimental curve towards the selected reference curve.

If τ_{rm} of Eq. (3) obeys Eq. (7), then isothermal $D(t, \sigma)$ can be expressed as

$$\begin{aligned} \log D(t, \sigma) &= [\log W(\sigma) - n \log \tau_{rmi} - n \log a_\varepsilon(t)] + n \log t \\ &= \log C(t, \sigma) + n \log t \end{aligned} \quad (9)$$

To separate the effects of stress and time, Eq. (9) can be rewritten in the following form:

$$\begin{aligned} \log D(t^*, \sigma) &= [\log W(\sigma) - n \log \tau_{rmi}] + n[\log t - \log a_\varepsilon(t)] \\ &= \log C^*(\sigma) + n^* \log t^* \end{aligned} \quad (10)$$

where parameters C^* and n^* are related to internal time t^* which reads:

$$\begin{aligned} \log t^* &= \log t + (B/2.303) \\ &\times \frac{[(1 - 2\nu)M\varepsilon(t)/(f_g + \Delta f_{T_c})]}{[(1 - 2\nu)M\varepsilon(t) + (f_g + \Delta f_{T_c})]} \end{aligned} \quad (11)$$

The $\log D(t)$ vs. $\log t$ plot would coincide with the $\log D(t^*)$ vs. $\log t^*$ plot for extremely low stresses and strains, for which $\Delta f_\varepsilon \rightarrow 0$; thus C^* and n^* are the limiting values of C and n for the creep in a (hypothetical) pseudo iso-free volume state. Eq. (10) anticipates a linear dependence of $\log D(t^*)$ vs. $\log t^*$, which, however, has nothing to do with the linear viscoelasticity. Alternatively, to characterize some long-term $\log D(t^*)$ vs. $\log t^*$ dependencies, e.g. of poly(ethylene terephthalate) and of its blends with impact modifiers, a polynomial of the second degree [31] was to be used:

$$\log D(t^*, \sigma) = \log C^*(\sigma) + (a^* + b^* \log t^*) \log t^* \quad (12)$$

2.3. Strain magnification factor for the amorphous phase in crystalline polymers

As the crystalline phase has distinctly lower compliance than the amorphous phase at $T > T_g$, the viscoelastic processes underlying the creep in crystalline polymers at $T > T_g$ take mainly place in the amorphous phase. The percolation theory shows [50–53] that the critical volume fraction (percolation threshold) of a component (phase) consisting of single-size spheres is about $v_{cr} = 0.156$. Thus the co-continuity of amorphous and crystalline phases is obvious in polypropylenes with crystallinity attaining 35–50%. A dual phase structure can be visualized in a simplified manner by a two-parameter equivalent box model (EBM) (Fig. 1), which was successfully used in the predictive formats for the moduli, yield strength, permeability, etc. [54–58] of two-component heterogeneous materials.

To account for differing strains of amorphous (subscript 1) and crystalline (subscript 2) phases in the EBM, the strain-magnifying factor M can be introduced as the mean ratio of the actual (microscopic) strain of the amorphous phase and the measured (macroscopic) strain of the specimen [3]. If a crystalline polymer is deformed, the strain of the amorphous and crystalline fractions coupled in parallel, i.e. v_{1p} and v_{2p} , is identical with the measured strain. On the other hand, if the crystalline phase has the compliance by 2–3 orders of magnitude lower than the amorphous phase above its T_g , it is evident that the crystalline fraction v_{2s} (Fig. 1) coupled in series is not perceptibly deformed in the course of the creep. As the displacement in the fraction v_{1s} is equal to the macroscopic displacement, the resulting strain of the amorphous phase coupled in series is higher than the measured strain; consequently, the generation of the strain-induced free volume

in the fraction v_{1s} will be higher than in the fraction v_{1p} . As we have shown, [3,29,30] the mean value of M for the amorphous phase is

$$M = 1 + \left(\frac{v_{2s}}{v_1} \right) \quad (13)$$

Utilizing a universal formula for the elastic modulus (or compliance) proposed by the percolation theory [50–53] for heterogeneous binary systems, we have derived [54–58] the following equations for the volume fractions of the EBM:

$$v_{1p} = \left[\frac{v_1 - v_{1cr}}{1 - v_{1cr}} \right]^q \quad (14a)$$

$$v_{2p} = \left[\frac{v_2 - v_{2cr}}{1 - v_{2cr}} \right]^q \quad (14b)$$

where v_{1cr} and v_{2cr} are the critical volume fractions and q is the critical universal exponent. As the EBM in Fig. 1 is a two-parameter model, only two of the four volume fractions are independent. The fractions v_{1s} and v_{2s} can be calculated by using the following relations:

$$v_{1s} = v_1 - v_{1p} \quad (15a)$$

$$v_{2s} = v_2 - v_{2p} \quad (15b)$$

Values of q were mostly reported [51–55] in an interval of 1.6–2.0 so that $q = 1.8$ may be used as a typical value. Considering PP as a two-phase system, we have used $v_{1cr} = v_{2cr} = 0.156$ and $q = 1.8$ for approximate calculations of the parameter M .

3. Experimental section

3.1. Tested polypropylenes

Some properties of tested polypropylenes are summarized in Table 1. In brief, Mosten 58.412 is isotactic polypropylene produced by Chemopetrol, Litvínov, Czech Republic. The other species are products of Basell, Ferrara, Italy. Moplen EPT30R is a blend consisting of 88% of isotactic polypropylene and 12% of ethylene/propylene rubber (EPR). This rubber-toughened polypropylene (RTPP) is prepared by a two-step polymerization reaction so that spherical domains of EPR are evenly distributed in PP matrix and bound by covalent bonds [58]. Moplen C30G is isotactic polypropylene recommended for the production of injection-molded products. Moplen RP210G is a random copolymer with 3% of ethylene designed for blow molding and sheet extrusion. Moplen HP500H is a homopolymer suitable for extrusion and injection molding. Moplen EP548S is a high-melt-flow-rate heterophase polypropylene copolymer mainly intended for thin wall injection molding. Preparation of injection-molded dumb-bell test specimens (ISO 527) was described in previous papers [3,12,29–31,62,63].

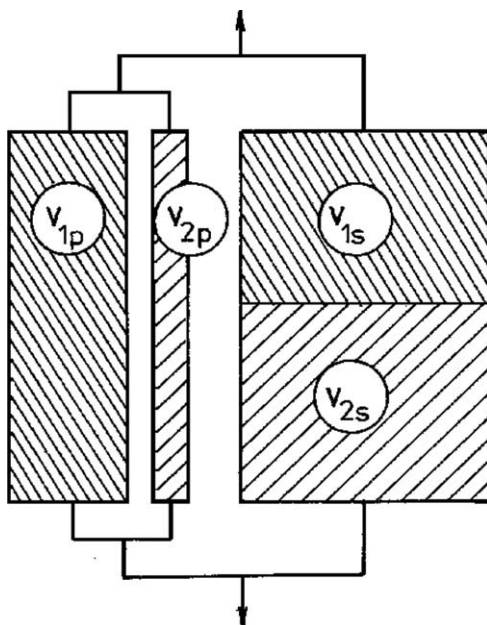


Fig. 1. Equivalent box model (EBM) for a two-component system (schematically).

Table 1
List of studied polypropylenes

Product	Code	MFI ^a (g/10 min)	Density (g/cm ³)	T_m^b (°C)	X_1^c (%)	X_2 (%) ^d	LP (nm) ^e	M^f
Mosten 58412	PP1	3	0.9065	173.1	48.4	50.7	13.1	1.59
Moplen EP548S	PP2	44	0.9037	168.3	46.3	47.8	13.8	1.57
Moplen HP500H	PP3	1.8	0.9046	167.2	44.4	46.1	14.9	1.54
Moplen C30G	PP4	6	0.9043	166.9	44.4	46.3	13.8	1.54
Moplen EPT30R	PP5	3.5	0.8994	167.9	39.8	42.2	13.1	1.49
Moplen RP210G	PP6	1.8	0.8912	151.3	36.5	38.4	12.2	1.40

^a Melt flow index at 230 °C and a load of 2.16 kg.

^b Melting temperature in the first DSC scan (for details on the method see Ref. [59]).

^c Crystallinity in the first DSC scan by using $\Delta H = 207$ J/g [60].

^d Crystallinity in the second DSC scan.

^e Long period from WAXS [61].

^f Strain magnification factor from Eq. (13).

3.2. Tensile creep measurements

Tensile creep was measured by using an apparatus equipped with a mechanical stress amplifier (lever) 10:1. A mechanical strain gauge (with an accuracy of about 2 μm) was connected with the upper clamp of the specimen to indicate the displacement. Specimen dimensions: initial distance between grips 90 mm; cross-section 10 mm \times 4 mm. Specimens were stored and creep tests were implemented at 23 ± 1 °C, i.e. about 30 K above T_g of PP. Short-term measurements in the interval 0.1–100 min were performed at five stress levels with one test specimen; each measurement was followed by a 22 h recovery before another creep test (at a higher stress) was initiated. Test specimens were used only once for long-term creep measurements in the interval 0.1–10,000 min. Specimens for creep studies were stored for at least 6 months at room temperature to exclude possible interfering effect of physical aging during creep measurements. Mechanical preconditioning preceding the series of short-term creeps consisted in applying a stress (for 100 min) equal to or higher than the highest stress applied in the series of creep measurements. Long-term measurements were preceded by application of a stress, which produced within 100 min a strain larger than the expected final strain of the intended experiment; the following recovery (before the registered creep was initiated) was about 24 h.

4. Results and discussion

4.1. The time-tensile strain superposition of short-term compliance dependencies acquired for different stresses

The stress-strain linearity is evidenced by the coincidence (overlapping) of the compliance curves acquired for different stresses. To this end we have selected PP6 characterized by a more pronounced viscoelastic behavior due to lower crystallinity. Fig. 2(a) including the short-term creeps of PP6 (Table 2) shows that increasing stress accounts for (i) an increase in $D(t, \sigma)$ and (ii) an increase in the derivative $d \log D(t, \sigma) / d \log(t)$ with the elapsed time of creeping. Analogous features revealing the non-linear viscoelastic

behavior were also observed for the other PPs. Obviously, the as-measured compliance curves for different stresses cannot be superposed by means of simple shifts along the axes. An alternative superposition procedure consists in plotting the compliance data against the internal time t^* . Although it is quite clear how the shift factor $\log a_\epsilon(t)$ is to be calculated, a crucial problem is the availability, reliability and accuracy of the input data, i.e. B , f_g , α_{fv} , M and $\nu(\epsilon, t)$. As indicated by Eqs. (10) and (11), these inputs affect the final shape of the superposed dependence and its location on the time scale. The value of B is believed—with regard to its definition—to be a constant close to 1. However, lower or higher values of B were reported, namely $0.5 < B < 1$ [64] or $2.3 < B < 3.2$ [25]. The fractional free volume in the glassy state $f_g = 0.025$ is generally taken as an average universal constant. This value seems to be also appropriate for the amorphous phase of crystalline polymers because a fractional free volume of about 0.03 was reported [35] for amorphous parts of PP. Similarly, the coefficients of thermal expansion below and above T_g seem to be only slightly affected by PP crystallinity [35]. The strain-magnifying factor M defined by Eq. (13) is an approximation because it corresponds to an average value calculated under simplified conditions disregarding possible distribution of local strains.

Equally difficult problems are related to Poisson's ratio of thermoplastics and to its possible dependencies on strain and/or time. Recent paper [65] has shown that the time-dependent Poisson's ratio $\nu(t)$ should be determined in the longitudinal direction in response to a step function of time, i.e. in a stress relaxation. Respecting this condition, a relatively simple equation was derived for $\nu(t)$ of the standard linear solid (SLS). It was accentuated that the derived equation should not be used where a 'good approximation' to an infinitesimally small deformation cannot be assumed. A related function proposed [65] for time-dependent Poisson's ratio in creep experiments was later found incorrect [28]. Although Poisson's ratio is indispensable for rigorous description of mechanical properties of polymeric materials, sporadic data occurring in the literature are often uncertain due to questionable methods of measurement. Epoxies and rubber-modified epoxies showed

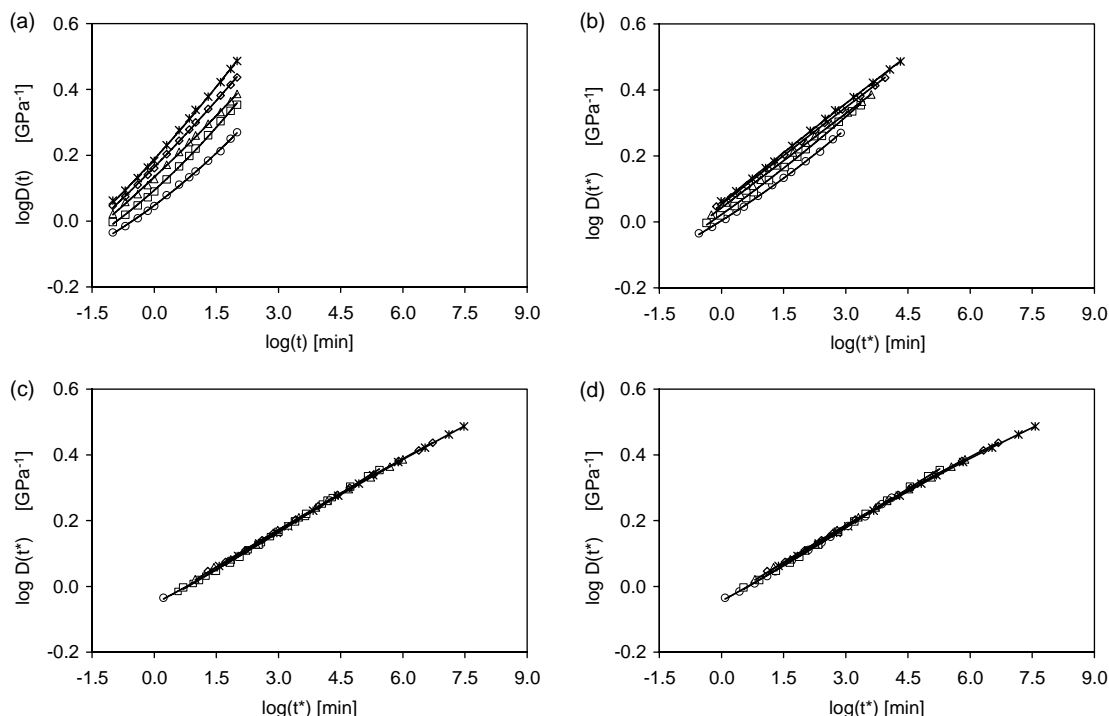


Fig. 2. Effect of stress on the $\log D(t)$ vs. $\log t$ dependencies in short-term tensile creep of polypropylene PP6. Applied stress (in MPa): (\circ) 7.32; (\square) 9.76; (\triangle) 10.98; (\diamond) 12.20; (\times) 13.42. Factor $M=1.40$. (a) Data plotted against real time $\log t$; (b) data plotted against internal time $\log t^*$ calculated for $B=1$, $(f_g + \Delta f_{T_c}) = 0.035$ and $\nu=0.43$; (c) data plotted against internal time $\log t^*$ calculated for $B=1$, $(f_g + \Delta f_{T_c}) = 0.025$ and $\nu=0.40$; (d) data plotted against internal time $\log t^*$ calculated for $B=2.4$, $(f_g + \Delta f_{T_c}) = 0.035$ and $\nu=0.43$.

a virtually linear increase in the volume with tensile strain in the region of reversible deformation [66], which indicates a constant ν . In creep experiments, polycarbonate [67], poly(methyl methacrylate) [67] and plasticized epoxies [68] exhibited a small increase in ν with tensile deformation. Tensile creep of poly(vinyl chloride) indicated the rise of $\nu(\varepsilon, t)$ with time and applied stress in the interval $0.39 < \nu(\varepsilon, t) < 0.45$ [66]. However, only constant values of ν are usually tabulated to characterize polymers [1,7,11].

In the first attempt to implement the internal time—tensile compliance superposition of PPs, we will consider the following values found in the literature: $T_g = 266$ K [8], $\alpha_1 - \alpha_g = \alpha_{fv} = 3.3 \times 10^{-4} \text{ K}^{-1}$ [60]. As no specific data are available for PP, $B=1$ will be introduced. For simplicity, also Poisson's ratio will be taken as constant, i.e. $\nu=0.4$ [1] or 0.43 [69]. Employing the versatile value $f_g = 0.025$, we obtain $(f_g + \Delta f_{T_c}) = 0.025 + 3.3 \times 10^{-4} \text{ K}^{-1} (296 - 266 \text{ K}) \cong 0.035$. The values of M calculated for $\nu_{1cr} = \nu_{2cr} = 0.156$ and $q=1.8$ using Eq. (13) are given in Table 1. Fig. 2(b) shows that the creep data for different stresses do not superpose, presumably owing to the inaccuracy (inadequacy) of the available input data. Thus it is important to see whether the superposition can be improved through an appropriate adjustment of some inputs. The criteria for the selection of a suitable set of the inputs can be defined as follows: (i) selected inputs are in a reasonable accord with reported (but often questionable) data; (ii) short-term compliance dependencies obtained for five different stresses superpose to form a smooth generalized dependence in

the $\log D(t^*)$ vs. $\log t^*$ coordinates; (iii) this generalized dependence coincides with an experimentally determined long-term dependency.

Inspecting Eq. (8) one can see that an increase in $(f_g + \Delta f_{T_c})$ can be compensated by a decrease in ν ; similarly, an increase in B permits to increase $(f_g + \Delta f_{T_c})$ and ν . Thus it seems that equivalent improvements in the superposition can be attained via several adjustments of the input parameters. To prove or disprove this possibility, we have selected $B=1$ and empirically found that the superposed curve is quite smooth for $(f_g + \Delta f_{T_c}) = 0.025$ and $\nu=0.4$ (Fig. 2(c)). Vice versa, if reported values $(f_g + \Delta f_{T_c}) = 0.035$ and $\nu=0.43$ [69] are kept and $B=2.4$ is empirically adjusted, a virtually equivalent generalized dependence is obtained (Fig. 2(d)). However, the latter value of B may not be realistic so that we will use the first data set for all studied PPs. Fig. 2(c) and (d) reveal an important fact that even though the superposition is attained with different series of inputs, the shape of the generalized curve and its position on the internal time scale are virtually identical. In other words, it is not possible to arbitrarily anchor the generalized curve on the time scale by manipulating with the inputs, because the superposition is successful only in a 'reference state,' i.e. in a certain interval on the t^* scale. As the achieved superposition is obviously very good, our attempts for further perfection by introducing $\nu(\varepsilon, t)$ as a simple function of time or strain [65] were ineffective.

In Fig. 3(a), five short-term compliance dependencies of PP5 are superposed to reconfirm the quality of the procedure.

Table 2
Effect of stress on the parameters of Eqs. (10) and (12)

Test	MPa ^a	log C*	n*	R ^{2b}	log C _a *	a*	b*	R _a ^{2b}
Mosten 58412 (PP1)								
STC ^c	8.41	−0.2811	0.0723	0.9936	−0.2705	0.0528	0.0053	0.9994
	12.01	−0.2877	0.0745	0.9925	−0.2625	0.0472	0.0054	0.9997
	14.41	−0.3024	0.0784	0.9930	−0.2690	0.0503	0.0045	0.9988
	16.81	−0.3112	0.0788	0.9977	−0.2898	0.0640	0.0020	0.9991
	19.21	−0.2858	0.0762	0.9996	−0.2828	0.0746	0.0002	0.9996
Average	–	−0.2936	0.0760	–	−0.2749	0.0578	0.0035	–
ESD ^d	–	0.0126	0.0027	–	0.0111	0.0113	0.0029	–
GenCrv ^e	–	−0.2934	0.0764	0.9948	−0.2813	0.0668	0.0014	0.9962
LTC ^f	12.01	−0.2984	0.0794	0.9989	−0.2959	0.0779	0.0001	0.9989
Moplen EP548S (PP2)								
STC	7.53	−0.1986	0.0731	0.9933	−0.1854	0.0514	0.0056	0.9998
	10.04	−0.2107	0.0743	0.9953	−0.1925	0.0541	0.0041	0.9994
	12.54	−0.2018	0.0746	0.9971	−0.1791	0.0568	0.0027	0.9994
	13.80	−0.1997	0.0738	0.9985	−0.1837	0.0628	0.0015	0.9993
	15.05	−0.1866	0.0717	0.9988	−0.1716	0.0628	0.0011	0.9993
Average	–	−0.1995	0.0735	–	−0.1825	0.0576	0.0030	–
ESD	–	0.0086	0.0012	–	0.0077	0.0051	0.0019	–
GenCrv	–	−0.2020	0.0742	0.9960	−0.1945	0.0668	0.0010	0.9965
LTC	10.07	−0.2222	0.0769	0.9988	−0.2177	0.0779	0.0003	0.9988
Moplen HP500H (PP3)								
STC	7.23	−0.1557	0.0741	0.9953	−0.1437	0.0544	0.0046	0.9998
	9.64	−0.1618	0.0746	0.9972	−0.1480	0.0602	0.0027	0.9991
	12.05	−0.1829	0.0773	0.9966	−0.1601	0.0696	0.0027	0.9988
	13.26	−0.1542	0.0744	0.9992	−0.1452	0.0678	0.0009	0.9995
	14.46	−0.1420	0.0714	0.9996	−0.1397	0.0701	0.0002	0.9997
Average	–	−0.1593	0.0744	–	−0.1473	0.0644	0.0022	–
ESD	–	0.0150	0.0021	–	0.0077	0.0069	0.0017	–
GenCrv	–	−0.1607	0.0745	0.9946	−0.1557	0.0706	0.0006	0.9949
LTC	12.01	−0.1764	0.0756	0.9985	−0.1859	0.0812	−0.0006	0.9987
Moplen C30G (PP4)								
STC	8.58	−0.2334	0.0814	0.9934	−0.2170	0.0578	0.0058	0.9998
	10.30	−0.2152	0.0813	0.9954	−0.1935	0.0584	0.0044	0.9999
	12.26	−0.2085	0.0813	0.9981	−0.1933	0.0691	0.0019	0.9991
	13.08	−0.2063	0.0786	0.9989	−0.2081	0.0798	−0.0002	0.9989
	15.94	−0.2027	0.0766	0.9996	−0.2063	0.0787	−0.0002	0.9996
Average	–	−0.2132	0.0798	–	−0.2036	0.0696	0.0023	–
ESD	–	0.0122	0.0022	–	0.0102	0.0108	0.0027	–
GenCrv	–	−0.2163	0.0804	0.9938	−0.2197	0.0831	−0.0004	0.9939
LTC	9.81	−0.2027	0.0793	0.9979	−0.2219	0.0887	−0.0009	0.9985
Moplen EPT30R (PP5)								
STC	7.82	−0.1530	0.0798	0.9959	−0.1394	0.0609	0.0043	0.9997
	9.78	−0.1449	0.0795	0.9958	−0.1277	0.0629	0.0030	0.9982
	11.00	−0.1572	0.0808	0.9983	−0.1426	0.0685	0.0019	0.9993
	12.23	−0.1528	0.0809	0.9992	−0.1463	0.0763	0.0006	0.9994
	13.45	−0.1346	0.0778	0.9997	−0.1388	0.0793	−0.0002	0.9997
Average	–	−0.1485	0.0798	–	−0.1390	0.0696	0.0019	–
ESD	–	0.0089	0.0012	–	0.0070	0.0087	0.0018	–
GenCrv	–	−0.1504	0.0802	0.9975	−0.1461	0.0767	0.0005	0.9976
LTC	7.32	−0.1512	0.0825	0.9989	−0.1531	0.0840	−0.0002	0.9987
Moplen RP210G (PP6)								
STC	7.82	−0.0601	0.0756	0.9987	−0.0532	0.0668	0.0019	0.9995
	9.76	−0.0651	0.0773	0.9993	−0.0602	0.0738	0.0007	0.9994
	10.98	−0.0493	0.0732	0.9993	−0.0571	0.0787	−0.0008	0.9995
	12.20	−0.0474	0.0727	0.9994	−0.0599	0.0803	−0.0009	0.9990
	13.42	−0.0725	0.0504	0.9994	−0.0659	0.0807	−0.0009	0.9998
Average	–	−0.0589	0.0698	–	−0.0593	0.0761	0.0000	–
ESD	–	0.0106	0.0110	–	0.0047	0.0058	0.0012	–
GenCrv	–	−0.0547	0.0740	0.9987	−0.0628	0.0798	−0.0008	0.9991
LTC	7.38	−0.0736	0.0751	0.9984	−0.0835	0.0822	−0.0008	0.9988

^a Tensile stress in MPa.

^b Reliability values.

^c Short-term creep (100 min).

^d Estimated standard deviation.

^e Parameters of the generalized compliance curve obtained by fitting the data from five STC.

^f Long-term creep (more than 10,000 min).

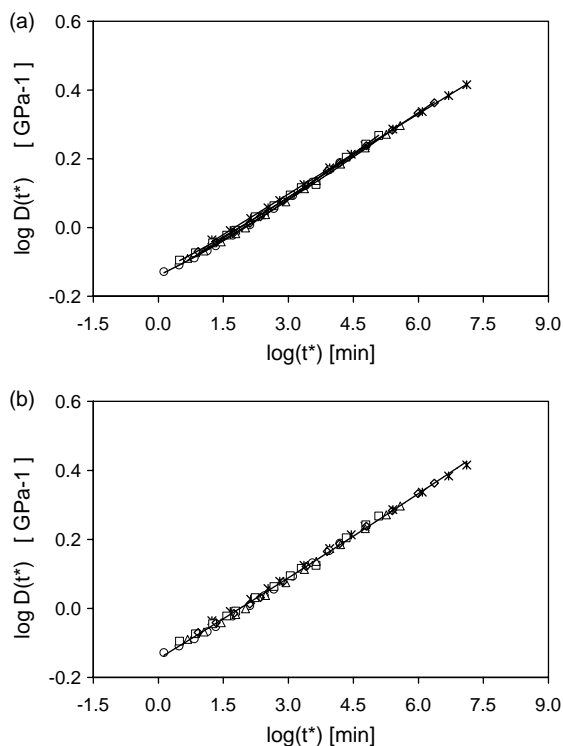


Fig. 3. Superposition of the short-term $\log D(t^*)$ vs. $\log t^*$ dependencies of polypropylene PP5, applied stress (in MPa): (○) 7.82; (□) 9.78; (△) 11.00; (◇) 12.23; (×) 13.45. Data plotted against internal time $\log t^*$ calculated for $M=1.49$, $B=1$, $(f_g + \Delta f_{T_c})=0.025$ and $\nu=0.40$. (a) Data for each stress approximated by a straight line; (b) all data approximated by one straight line (cf. Table 2).

In parallel, all plotted experimental data are approximated by one generalized curve in Fig. 3(b). Read-off parameters of Eqs. (10) and (12) used for fitting both types of experimental dependencies of six studied PPs are summarized in Table 2 where also the parameters for long-term experiments (lasting over 10,000 min) are given. Hence it is evident that the fitting of experimental data by Eq. (10) or Eq. (12) is equally good for all types of PP. The average values of parameters (resulting from five short-term measurements) are very close to those characterizing the corresponding generalized dependence, which proves correctness of the applied superposition procedure. The differences between the reliability parameters R^2 and R_a^2 found for individual generalized dependencies are virtually negligible, which implies that simpler Eq. (10) is fully satisfactory for all types of PP. Eq. (12) permits somewhat better fitting of experimental data but ESD (estimated standard deviation) for a^* and particularly for b^* are much higher than ESD for n^* . Very low values of b^* evidence only small deviations from linearity of the $\log D(t^*)$ vs. $\log t^*$ dependencies; thus it seems that Eq. (12) solely better reflects possible irregularities in individual dependencies. The average values of $\log C^*$ are systematically somewhat lower than the values of $\log C_a^*$, which can be ascribed to the fact that Eq. (10) almost ignores possible irregularities in the read-off displacements shortly after the load imposition. Table 2 also evidences that no clear-cut dependencies of $\log C^*$ and n^* on stress can be

observed, which is in conformity with the concept that $\log C^*$ and n^* are the limiting values for creep in the pseudo iso-free volume state.

4.2. Comparison of short- and long-term compliance dependencies

Long-term creep measurements are summarized in Fig. 4 and Table 2 indicating some differences between the studied PPs: while the compliance of PPs rises with decreasing crystallinity (Table 1), the differences between the slopes n^* of the $\log D(t^*)$ vs. $\log t^*$ dependencies are very small except for PP5, whose slightly higher n^* is probably caused by dispersed rubbery component [58]. Some long-term dependencies seem to be slightly S-shaped, yet they can be plausibly approximated by Eq. (10). Fig. 5 brings three examples evidencing that the short-term $\log D(t^*)$ vs. $\log t^*$ dependencies at elevated stresses almost perfectly coincide with a corresponding long-term dependency found for a lower stress. The parameters of the superposed and experimental long-term dependencies are in a very good concurrence for all tested PPs (Table 2), thus indicating that a series of short-term creeps can be an effective substitute for a long-term measurement. All these results validate the outlined superposition principle and the selection of the inputs.

As can be seen, the compliance dependencies determined in the region of non-linear viscoelasticity can be superposed over the whole measured time intervals if they are reconstructed for a constant (initial) free volume. In other words, non-linear creep behavior becomes apparently linear if the coordinates $\log D(t^*, \sigma)$ vs. $\log t^*$ are introduced. Obviously, such generalized dependencies cannot be obtained experimentally because the deformations for $\Delta f_e \rightarrow 0$ would be infinitesimally small and the time of measurements beyond the laboratory possibilities. The results of this and our previous papers [3,28–31] allow to assume that the main reason for the non-linear tensile creep of materials with Poisson ratio $\nu < 0.5$ can be sought in the strain-induced dilatation. Molecular mobility

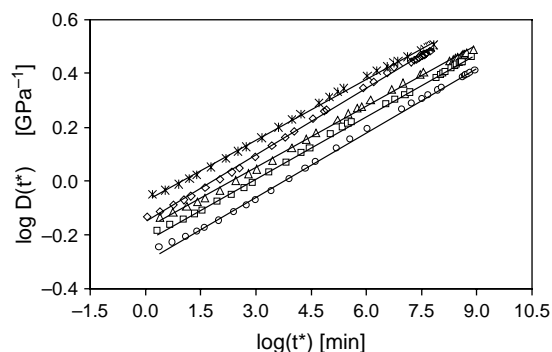


Fig. 4. The $\log D(t^*)$ vs. $\log t^*$ dependencies for long-term tensile creep of studied polypropylenes. Type of PP (Table 1) and applied stress (in MPa): (○) PP1, 12.01; (□) PP2, 10.07; (△) PP3, 9.64; (◇) PP5, 7.32; (×) PP6, 7.38. The dependence for PP4 (not given) coincides with that for PP3. All data are plotted against internal time $\log t^*$ calculated for $B=1$, $(f_g + \Delta f_{T_c})=0.025$ and $\nu=0.40$; values M are given in Table 1.

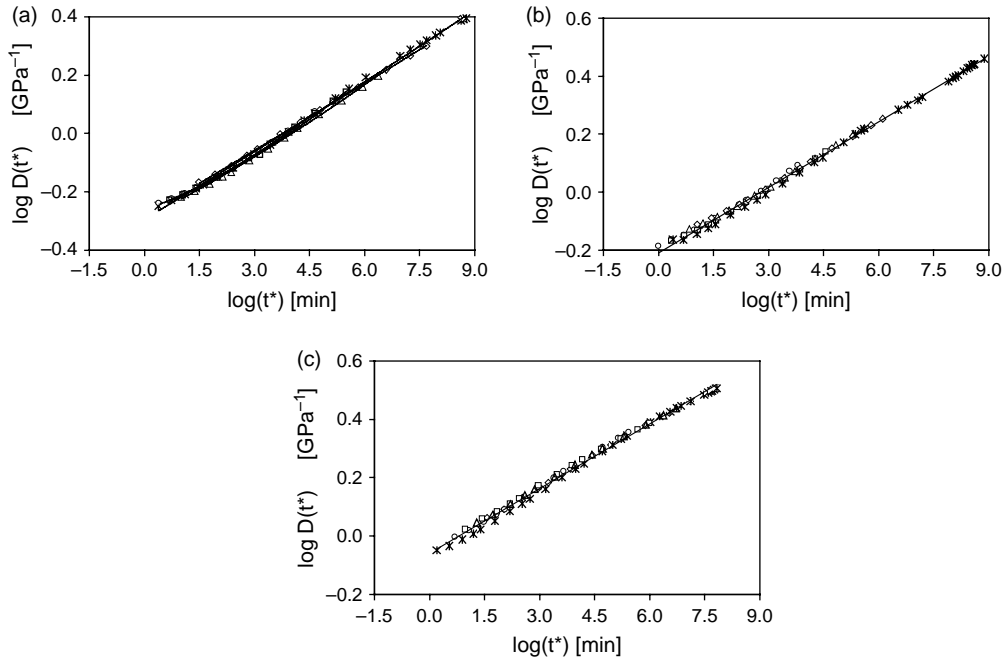


Fig. 5. Comparison of the generalized curve obtained through the time-strain superposition of four short-term creeps (STC) with the experimental long-term creep curve (LTC). Data are plotted against internal time $\log t^*$ calculated for $B=1$, $(f_g + \Delta f_{T_c}) = 0.025$ and $\nu=0.40$; values M are given in Table 1. All data in each figure approximated by one straight line. Type of PP (Table 1) and applied stresses (in MPa): (a) PP1-STC: (\circ) 12.01; (\square) 14.41; (\triangle) 16.81; (\diamond) 19.21; LTC: (\times) 12.01. (b) PP2-STC: (\circ) 7.53; (\square) 10.04; (\triangle) 12.54; (\diamond) 13.80; LTC: (\times) 10.07. (c) PP6-STC: (\circ) 9.76; (\square) 10.98; (\triangle) 12.20; (\diamond) 13.42; LTC: (\times) 7.38.

increased due to strain-induced free volume increment Δf_ε reduces the material resistance to deformation (i.e. enhances the compliance), which in turn facilitates further growth of strain and, consequently, of Δf_ε . This ‘autocatalytic’ process accounts for a steady acceleration of the running creep. However, this effect will hardly be detectable in two specific cases: (1) at very small stresses and produced strains, for which Δf_ε remains negligible in comparison with $(f_g + \Delta f_{T_c})$; (2) as indicated by Eq. (5), Δf_ε decreases as ν approaches 0.5, which is typical of materials close to or in the rubber-like state.

The outlined calculations show that if all material parameters (B , f_g , α_{fv} , M and ν) are kept constant then the resulting stress-strain relationship is non-linear (compliance rises with stress). A linear relationship (compliance independent of stress) would require that some of the material parameters spontaneously vary with stress (or strain) in an exactly predefined way to transform non-linearity into linearity. As such a ‘compensation law’ would be very fortuitous (obviously, all other ways of the variations of the material parameters would preserve non-linearity), the non-linear viscoelastic behavior should be viewed as general, while linear behavior as a specific case. The existing concept of the linearity limit implies that there is a ‘break’ in some material parameters, which gives rise to markedly differing viscoelastic properties below and above this limit. With regard to recent results, such a limit is to be viewed as an arbitrary artificial limit obviously depending on the accuracy of the used methods, namely the higher the method accuracy the lower the observed linearity limit.

4.3. Calculation of the time-dependent real compliance from the generalized dependency

A practical outcome of the proposed format is that the generalized $\log D(t^*)$ vs. $\log t^*$ dependency can be utilized for calculating the real $\log D(t)$ vs. $\log t$ curves for selected stresses. The procedure employs experimentally found constants $\log C^*$ and n^* (Table 2), which allow to calculate compliance $D(t^*)$ for any selected ‘internal’ time t^* . To obtain the corresponding ‘real’ time t we can modify Eq. (8) by introducing $\varepsilon(t) = \sigma D(t)$:

$$\log a_\varepsilon = -(B/2.303) \frac{[(1-2\nu)M\sigma D(t)/(f_g + \Delta f_{T_c})]}{[(1-2\nu)M\sigma D(t) + (f_g + \Delta f_{T_c})]} \quad (16)$$

As Eq. (11) shows that

$$\log t = \log t^* + \log a_\varepsilon \quad (17)$$

a series of data points of the $\log D(t)$ vs. $\log t$ dependency can be calculated for a selected constant tensile stress. In Fig. 6, three examples of the long-term compliance for $\sigma=4.84$ or 8.54 or 12.09 MPa are calculated and compared with experimental curves of PP5. The values of $\log C^*$ and n^* used in the calculations were extracted from the short-term creeps (Table 2); the other inputs were identical with those used in the superposition procedure. The compliance curves calculated for $\sigma=4.84$ and 8.54 MPa fit experimental curve quite well up to $\log t=4.2$. For the highest applied stress $\sigma=12.09$ MPa, the resistance to creep is seemingly underestimated; the discrepancy can tentatively be attributed to

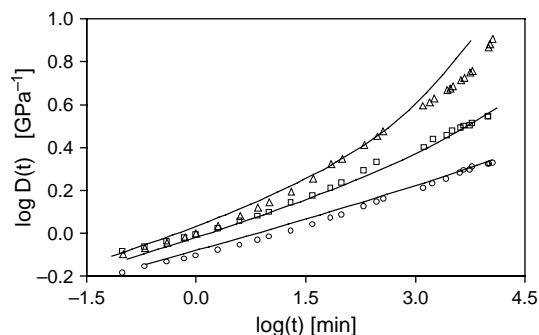


Fig. 6. Comparison of long-term experimental (data points) and predicted compliance curves (full lines) of PP5. Input parameters (Table 2): $\log C^* = -0.1485$; $n^* = 0.0798$; $B = 1$; $M = 1.49$; $(f_g + \Delta f_{T_c}) = 0.025$; $\nu = 0.4$. Applied stress (in MPa) in long-term creep experiments: (○) 4.84; (□) 8.54; (△) 12.09.

some structure orientation (strain hardening) in the creeping specimen because the final strain attained 9.8% (it is to be mentioned that analogous curves calculated by means of $\log C_a^*$, a^* and b^* are prone to substantial deviations from reality for long times of creeping, probably owing to insufficiently accurate values of b^*). Fig. 6 demonstrates that the discussed uncertainties in the input data do not preclude a fairly good prediction of compliance curves if the input parameters are identical with those used in the time-strain superposition.

5. Conclusions

The free-volume theory of viscoelasticity was used to develop the tensile compliance vs. internal time superposition in the region of non-linear viscoelastic behavior of polypropylenes. The used concept assumes that the non-linearity is mainly caused by the strain-induced increment of the free volume, which is typical of materials with Poisson's ratio smaller than 0.5. The outlined calculations show that if all material parameters are kept constant then the resulting stress-strain relationship is non-linear (compliance rises with stress). Thus the linearity limit is to be viewed as an arbitrary artificial limit obviously depending on the accuracy of the used methods, namely the higher the method accuracy the lower the observed linearity limit.

The strain-induced additional free volume rises with creep strain and accounts for shortening of retardation times. To implement the time-strain superposition of non-linear creep data, the shift factors are to be calculated a priori point by point for superposed compliance dependencies. A function continuously rising with the creep strain was derived for the shift factor along the internal time scale to obtain a generalized creep curve (over extended time scale) corresponding to a pseudo iso-free-volume state. The generalized curve can be generated by means of short-term creep tests at a series of elevated stresses, which leads to essential time saving. The proposed superposition procedure was found viable for all studied types of PP and

the validity of the generalized compliance curves was proved by their coincidence with experimental long-term curves.

The compliance dependencies for the pseudo iso-free-volume state should be used for the comparison of the creep behavior of various materials to eliminate the effects of unequal strain and generated additional free volume. The results show that the compliance of PPs decreases with their crystallinity, while the $\log D(t^*)$ vs. $\log t^*$ dependency is virtually linear and its slope (i.e. creep rate) is almost identical for all PPs. Only rubber-toughened PP does show a slightly steeper increase in compliance with time, which can be attributed to the 'softening' effect of rubber particles evenly distributed in the PP matrix. A most practical outcome of the outlined format is that the generalized $\log D(t^*)$ vs. $\log t^*$ dependency can be used for calculating a long-term $\log D(t)$ vs. $\log t$ dependency for any selected stress (in the interval up to the yield stress) at which no plastic deformation occurs.

Acknowledgements

The first author (J.K.) is greatly indebted to the Grant Agency of the Czech Republic for financial support of this work (Grant No. 106/04/1051). The authors are very grateful to Prof Luca Fambri for the data on crystallinity and density of studied polypropylenes and to Dr Josef Baldrian for the WAXS data on lamellar thickness.

References

- [1] Crawford RJ. *Plastics engineering*. Oxford: Butterworth-Heinemann; 1988.
- [2] Andrew W. *The effect of creep and other time related factors on plastics and elastomers*. New York: Plastics Design Library; 1991.
- [3] Kolařík J. *J Polym Sci, Part B: Polym Phys* 2003;41:736.
- [4] Bueche F. *Physical properties of polymers*. New York: Interscience; 1962.
- [5] Ferry JD. *Viscoelastic properties of polymers*. New York: Wiley; 1980.
- [6] Ward IM, Hadley DW. *An introduction to the mechanical properties of solid polymers*. Chichester: Wiley; 1993.
- [7] Nielsen LE, Landel RF. *Mechanical properties of polymers and composites*. New York: Marcel Dekker; 1994.
- [8] Rodriguez F. *Principles of polymer systems*. Washington, DC: Taylor & Francis; 1996.
- [9] Lakes RS. *Viscoelastic solids*. Boca Raton: CRC Press; 1999.
- [10] Riande E, Diaz-Calleja R, Prolongo MG, Masegosa RM, Salom C. *Polymer viscoelasticity*. New York: Marcel Dekker; 2000.
- [11] Moore DR, Turner S. *Mechanical evaluation strategies for plastics*. Cambridge: Woodhead Publ; 2001.
- [12] Kolařík J, Fambri L, Pegoretti A, Penati A, Goberti P. *Polym Eng Sci* 2002;42:161.
- [13] Popelar CF, Liechti KM. *Mech Time-Depend Mater* 2003;7:89.
- [14] Findley WN, Lai JS, Onaran K. *Creep and relaxation of nonlinear viscoelastic materials*. Amsterdam: North-Holland; 1976.
- [15] Turner S. *Polym Eng Sci* 1966;6:306.
- [16] Schapery RA. *Polym Eng Sci* 1969;9:295.
- [17] Knauss WG, Emri IJ. *Comput Struct* 1981;13:123.
- [18] Knauss WG, Emri I. *Polym Eng Sci* 1987;27:86.
- [19] Losi GU, Knauss WG. *Polym Eng Sci* 1992;32:542.
- [20] O'Dowd NP, Knauss WG. *J Mech Phys Solids* 1995;43:771.
- [21] McKenna GB, Leterrier Y, Schultheisz CR. *Polym Eng Sci* 1995;35:403.
- [22] Colucci DM, O'Connell PA, McKenna GB. *Polym Eng Sci* 1997;37:1469.

- [23] O'Connell PA, McKenna GB. *Polym Eng Sci* 1997;37:1485.
- [24] Lu H, Zhang X, Knauss WG. *Polym Compos* 1997;18:211.
- [25] Popelar CF, Liechti KM. *J Eng Mater Tech* 1997;119:205.
- [26] Lu H, Knauss WG. *Mech Time Mater* 1999;2:307.
- [27] O'Connell PA, McKenna GB. *Mech Time Mater* 2002;6:207.
- [28] Arzoumanidis GA, Liechti KM. *Mech Time-Depend Mater* 2003;7:209.
- [29] Kolařík J, Pegoretti A, Fambri L, Penati A. *J Appl Polym Sci* 2003;88:641.
- [30] Kolařík J, Pegoretti A, Fambri L, Penati A. *Macromol Mater Eng* 2003;288:629.
- [31] Pegoretti A, Kolařík J, Gottardi G, Penati A. *Polym Int* 2004;53:984.
- [32] Lai J, Bakker A. *Polymer* 1995;36:93.
- [33] Ferry JD, Stratton RA. *Koll Z* 1960;171:107.
- [34] Goyanes S, Salguero W, Somoza A, Ramos JA, Mondragon I. *Polymer* 2004;45:6691.
- [35] Kilburn D, Bamford D, Dlubek G, Pionteck J, Alam MA. *J Polym Sci, Part B: Polym Phys* 2003;41:3089.
- [36] Cho KS, Kim SY. *Macromol Theory Simul* 2000;9:328.
- [37] Cho KS, Kim SY. *Macromol Theory Simul* 2000;9:336.
- [38] Caruthers JM, Adolf DB, Chambers RS, Shrikhande P. *Polymer* 2004;45:4577.
- [39] Adolf DB, Chambers RS, Caruthers JM. *Polymer* 2004;45:4599.
- [40] Garbella RW, Wachter J, Wendorf JH. *Prog Colloid Polym Sci* 1985;71:164.
- [41] Read BE, Dean GD, Tomlins PE. *Polymer* 1988;29:2159.
- [42] Li XJ, Cheung WL. *J Appl Polym Sci* 1995;56:881.
- [43] Tomlins PE. *Polymer* 1996;37:3907.
- [44] Read BE, Tomlins PE. *Polym Eng Sci* 1997;37:1572.
- [45] Read BE, Tomlins PE. *Polymer* 1997;38:4617.
- [46] Tomlins PE, Read BE. *Polymer* 1998;39:355.
- [47] Schlimmer M. *Rheol Acta* 1979;18:62.
- [48] Kolařík J. *Adv Polym Sci* 1982;46:119.
- [49] McCrum NG, Read BE, Williams G. *Anelastic and dielectric effects in polymeric solids*. London: Wiley; 1967.
- [50] De Gennes PG. *J Phys Lett (Paris)* 1976;37:L1.
- [51] Sax J, Ottino JM. *Polym Eng Sci* 1983;23:165.
- [52] Hsu WY, Wu S. *Polym Eng Sci* 1993;33:293.
- [53] Lyngaae-Jorgensen J, Kuta A, Sondergaard K, Poulsen KV. *Polym Networks Blends* 1993;3:1.
- [54] Kolařík J. *Polym Eng Sci* 1996;36:2518.
- [55] Kolařík J. *Eur Polym J* 1998;34:585.
- [56] Kolařík J, Fambri L, Pegoretti A, Penati A. *Polym Eng Sci* 2000;40:127.
- [57] Kolařík J. *J Macromol Sci-Phys* 2000;B39:53.
- [58] Kolařík J, Pegoretti A, Fambri L, Penati A. *J Polym Res* 2000;7:7.
- [59] Kolařík J, Fambri L, Kruliš Z, Šlouf M. *Polym Eng Sci* 2005;45:817.
- [60] Van Krevelen DW. *Properties of polymers*. Amsterdam: Elsevier; 1997.
- [61] Baldrian J, Horký M, Sikora A, Steihart M, Vlček P, Amenitsch H, et al. *Polymer* 1999;40:439.
- [62] Raab M, Ščudla J, Kolařík J. *Eur Polym J* 2004;40:1317.
- [63] Šlouf M, Kolařík J, Fambri L. *J Appl Polym Sci* 2004;91:253.
- [64] Ito K, Saito Y, Yamamoto T, Ujihira Y, Nomura K. *Macromolecules* 2001;34:6153.
- [65] Tschoegl NW, Knauss WG, Emri I. *Mech Time Mater* 2002;6:3.
- [66] Stachurski ZH. *Prog Polym Sci* 1997;22:407.
- [67] Bertilson H, Delin M, Kubat J, Rychwalski WR, Kubat M. *J Rheol Acta* 1993;32:361.
- [68] Theocaris PS. *Polymer* 1979;20:1149.
- [69] Pegoretti A, Marini M, Pandini S. To be published.